Selective Hydrodefluorination of Hexafluoropropene to Industrially Relevant Hydrofluoroolefins

Nicholas A. Phillips, Andrew. J. P. White, Mark. R. Crimmin

Department of Chemistry, Molecular Sciences Research Hub, Imperial College London, 80 Wood Lane, London, W12 0BZ, UK.

Abstract: *The selective hydrodefluorination of hexafluoropropene to HFO-1234ze and HFO-1234yf can be achieved by reaction with simple group 13 hydrides of the form EH_3•L (E = B, Al; L = SMe_2, NMe_3). The chemoselectivity varies depending on the nature of the group 13 element. A combination of experiments and DFT calculations show that competitive nucleophilic vinylic substitution and addition-elimination mechanisms involving hydroborated intermediates lead to complementary selectivities*.

Introduction

Synthetic refrigerants have improved our quality of life and contributed the year-on-year growth of the fluorocarbon industry. [1] The most widespread synthetic refrigerants are volatile molecules of low molecular mass that contain at least one halogen atom. Refrigerants are applied in sealed compressor units in household refrigerators, climate control systems in cars or industrial air-conditioning units. Despite their immediate benefit to humanity, early generations of synthetic refrigerants and aerosols (CFCs and HFCs) have been a disaster for the environment. This led to legislation such as the Montreal Protocol restricting their use.[2,3] The fluorocarbon industry has responded by beginning the manufacture, marketing and supply of hydrofluoroolefins (HFOs). HFOs have global warming potentials similar to CO_2 and do not deplete ozone. These volatile molecules are our most advanced refrigerants and hold promise as a long-term solution to a long-standing environmental problem.[4]

The majority of known syntheses of industrially relevant HFOs rely on multistep processes involving partial chlorination of propane, halogen exchange to introduce the fluorine atom and a hydrodehalogenation step to obtain the olefin.[5-7] An approach involving the hydrogenation and hydrodefluorination of HFP has been reported using a chromium-based heterogeneous catalyst has also been reported.[8] Given that the majority of the patented industrial processes involve the redundant construction and destruction of a C–Cl bond along with toxic, corrosive and expensive materials, the selective hydrodefluorination of hexafluoropropene (HFP) is an attractive route to a number of commercially relevant HFOs including HFO-1234ze and HFO-1234yf (Figure 1). HFP itself is bulk commodity used in the manufacture of poly(fluoro)olefins.

Figure 1. Selective hydrodefluorination of HFP as a route to HFOs.

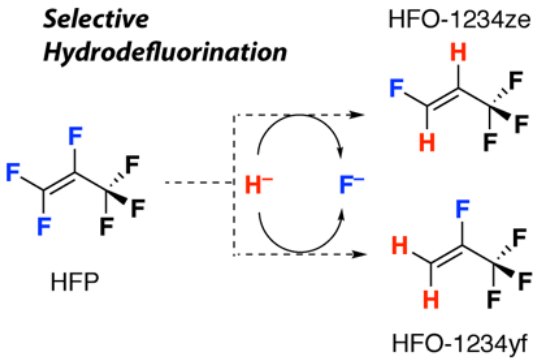

The selective hydrodefluorination of HFP to form tetrafluoroolefins has limited precedent. A number of researchers have shown that boranes react with fluoroolefins via either catalysed or non-catalysed pathways that can involve the generation of mixtures from a combination of hydroboration and hydrodefluorination steps.[9-13] Related alanes are also able to hydrodefluorinate these substrates. In 2018, it was reported that AlH_3•NHC (NHC = *N*-heterocyclic carbene) can selectively hydrodefluorinate HFP to form HFO-1234yf in 79% yield.[14,15]

Herein, we detail the hydrodefluorination of HFP to commercially relevant HFO-1234ze and HFO-1234yf. The selectivity can be guided by careful choice of Lewis base and group 13 hydride (EH_3•L; L = THF, SMe_2, NMe_3; E = B, Al). We show that the tailored and expensive *N*-heterocyclic carbene ligand systems are actually unnecessary for selective reactions. While these reactions rely on the use of stoichiometric quantities of the main group reagents, the by-products (EF_3•L) are industrially relevant materials in their own right. Through investigation of the mechanism we provide insight into the origin of selectivity and as such this work may act as a foundation for future (catalytic) routes from HFP to industrially relevant HFOs.

Results and Discussion

Hydrodefluorination of Hexafluoropropene: Surprisingly there are no reports investigating the reaction of hexafluoropropene (HFP) with the simple borane adducts BH_3•L (**1**, L = THF, SMe_2, NMe_3). Heating a sealed J Young NMR tube containing a solution of BH_3•SMe_2 in benzene-d_6 charged to 1 atm. of HFP at 100 °C forms isomers of 1,2,3,3,3-pentafluoropropene, *E*-**2** and *Z*-**2** after 24 h. Ultimately E-/Z-mixtures of 1,3,3,3-tetrafluoropropene (HFO-1234ze) are generated as the major product after heating for 5 d (Figure 2a).

Figure 2. Hydrodefluorination of HFP with (a) BH_3•L and (b) AlH_3•NMe_3.

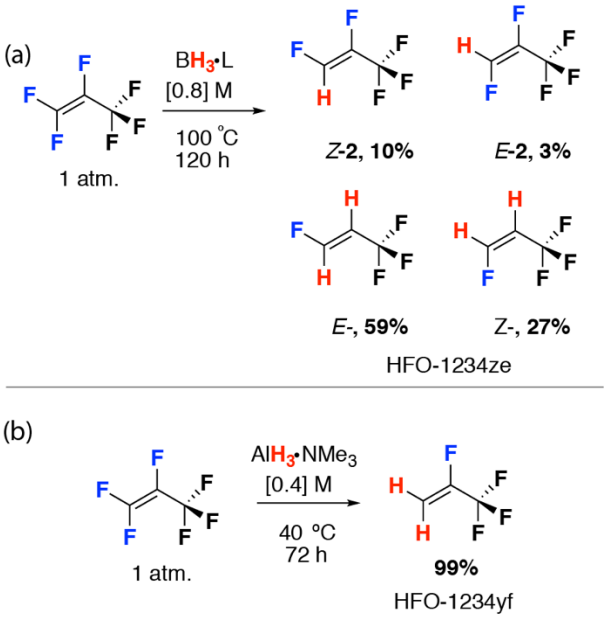

The final product distribution represents an 86% yield of HFO-1234ze formed in a 2:1 ratio of *E*:*Z* isomers. The remaining mass balance has been characterised as *E*/*Z*-**2** (13%) and trifluoropropene (<2%). The boron containing side-product contains diagnostic resonances in the ^{11}B and ^{19}F NMR spectra at δ_B = 3.2 (s) ppm, δ_F = –136.67 (br) ppm consistent with those reported for BF_3•SMe_2.

In contrast, the reaction of HFP with AlH_3•NMe_3 leads to the efficient and highly selective formation of 2,3,3,3-tetrafluoropropene (HFO-1234yf) under mild conditions in high yield and selectivity (1 atm. 40 °C, 72 h). Initial mixing of AlH_3•NMe_3 with HFP in benzene-d_6 results in rapid formation of a colourless precipitate (assumed to be AlF_3) and high conversion to *E*-**2** and *Z*-**2**, in ratio 2:1 as evidenced by ^1H NMR spectroscopy after 5 mins at 25 °C. Further HDF reactivity is observed even at ambient temperature, but warming the reaction to 40 °C gives optimum selectivity and rate, yielding HFO-1234yf as the major F-containing product (> 98%) after 72 h at 40 °C. Small quantities of 3,3,3-trifluoropropene (< 2%) are observed from over-reduction (Figure 2b).

Mechanisms of HDF: Several observations are consistent with the alane and borane reagents reacting by different pathways. The first of which is the ligand dependence of reactivity. Despite the strongly bound amine ligand, AlH_3•NMe_3 reacts readily and with the same selectivity as the AlH_3•NHC system. [14] In contrast, the borane system BH_3•L shows a strong ligand dependence with L = NMe_3 being ineffectual for HDF and L = THF highly inefficient. The latter borane was used as a THF solution and it is likely that exogeneous THF is acting as an inhibitor in the reaction. Only hydrocarbon solutions of BH_3•L L = SMe_3 proved a useful for HDF. The experiments are consistent with the borane reagents requiring a ligand dissociation step to react and the alane reagents not.

As part of detailed studies into the mechanism hydroboration with BH_3•L, Brown and co-workers have concluded that the reaction can be considered a combination of a reversible ligand dissociation step to form BH_3 followed by extremely facile addition to the alkene.[16,17] While solvent effects have historically been somewhat contentious in this field, the mechanism is now widely accepted. Brown and co-workers demonstrated that strong donor ligands, such as amines, decrease the rate of reaction.[16]

The second observation which would be consistent with a switch in mechanism is the switch in selectivity which is observed in changing the reagent from AlH_3•L to BH_3•L. The latter main group hydride gives a mixture of HFO-1234ze in low selectivity as the major product, while the former gives almost exclusively HFO-1234yf.

Alane Pathway (concerted S_NV): The hydrodefluorination of HFP with AlH_3•NMe_3 was observed to proceed without the formation of defined reaction intermediates. No experimental evidence was obtained to suggest that hydroalumination of the alkene occurs in the reaction mechanism. DFT calculations were used to probe the plausible pathways alongside a series of experiments investigating the formation and reactivity of reaction intermediates. Calculations were implemented in Gaussian09. A series of functionals ωB97xD, M06L, M062x, B3PW91-GD3BJ) were investigated to confirm that the trends were reproducible across a number of methods. While *all* the computational approaches led to the same qualitative outcomes for every single mechanism and reaction step, data for the B3PW91 functional are presented herein.

In line with the lack of a significant effect of the ligand L on reactivity, HDF was calculated to proceed by a concerted S_NV pathway involving the 4-coordinate aluminium reagent (Figure 3a-c). Formation of *E*-**2** is preferred over *Z*-**2** with activation barriers of $\Delta G^{‡}_{298K}$ = 24.8 and 27.7 kcal mol^{-1} respectively. *E*-**2** and *Z*-**2** can undergo a subsequent concerted HDF step with barriers of 28.3 and 28.2 kcal mol^{-1} respectively, both yielding HFO-1234yf. The calculations are consistent with the experimental data and predict the observation of pentafluoropropenes *E*-**2** and *Z*-**2** as intermediates due to the more challenging second HDF step, the preferential formation of intermediate *E*-**2**, and ultimately the high selectivity for the formation of HFO-1234yf. Ligand dissociation from AlH_3•NMe_3 is calculated to be exergonic by 22 kcal mol^{-1} and is not required for the cS_NV HDF pathway to operate. In fact, the lowest barriers for a direct HDF by the concerted pathway are already within a reasonable range of the ligand dissociation ΔG^{o} before considering any bond making or breaking steps involving AlH_3 and the fluoroolefin.

Transition states involving hydride transfer to the internal position of HFP, *E*-**2**, or *Z*-**2** are higher in energy ($\Delta G^{‡}_{298K}$ = 35 – 37 kcal mol^{-1}) than those for the terminal position ($\Delta G^{‡}_{298K}$ = 25 – 28 kcal mol^{-1}) and are unlikely to be accessible at 40 °C (Figure 3d). Similarly, the generation of 1,1,1-trifluoropropene by a 3rd HDF step of HFO-1234yf at the internal site occurs by a high energy transition state ($\Delta G^{‡}_{298K}$ = 36 kcal mol^{-1}). The relative barriers can be explained by considering the fluorinated substrates as Michael acceptors. In the cS_NV mechanism the CF_3 moiety acts as the electron-withdrawing group to activate the electrophile and the hydride takes the role of the nucleophile. Nucleophilic attack occurs with charge transfer to the fluorinated olefin. For attack at the terminal position, the transition state allows for negative charge accumulation at carbon centre adjacent to the CF_3 group. This charge is stabilised through inductive effects (–F and $–CF_3$) and destabilised through mesomeric effects (–F). For attack at the internal position the charge stabilisation is less pronounced. These effects are clear when comparing **TS-A1** and **TS-A3** (Figure 3e). In the former charge accumulation occurs at the centre adjacent to nucleophilic attack. Perturbation of the geometry of the carbon from sp^2 toward sp^3 hybridisation is evidenced by the average bond angles around this centre (**TS-A1**, Θ = 111.1°; **TS-A3**, Θ = 118.2°).

Hence, the HDF of HFP by a concerted S_NV mechanism involving a metal hydride reagent occurs with a substrate bias for the formation of HFO-1234yf in high selectivity. This realisation may set the foundation for routes from HFO to HFO-1234yf by catalytic hydrogenation and it is plausible that coordinatively saturated transition metal hydride complexes may behave in a similar manner to AlH_3•NMe_3.

Figure 3. DFT calculations for AlH_3•NMe_3 with (a) HFP, (b) *E*-PFP and (c) *Z*-PFP. (d) Comparison of TS geometries. (e) Comparison of *NPA* charges in the anionic fluoroalkene fragments of **TS-A1** and **TS-A3**. **alane** = AlH_3•NMe_3 by-product $AlFH_2$•NMe_3 not shown.

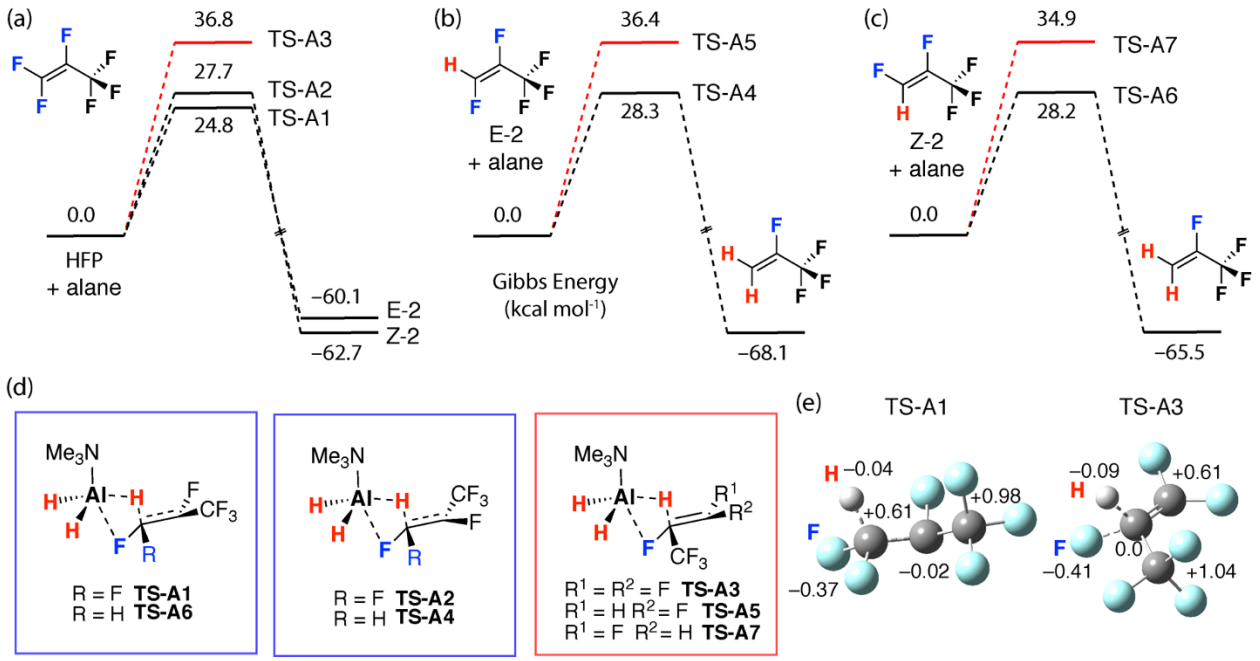

Borane Pathway (Addition-Elimination): The HDF of HFP by BH_3•SMe_2 did not lead to HFO-1234yf but rather a mixture of *E/Z*-isomers of HFO-1234ze. This reaction required more forcing conditions (100 °C for 5 d *versus* 40 °C for 3 d) to reach high conversion and proceeds with a lower selectivity than observed for the alane. Calculations show that the direct reaction of BH_3•SMe_2 with HFP by a concerted S_NV mechanism requires the formation prohibitively high energy transition states ($\Delta G^{\ddagger}_{298K}$ = 50 – 60 kcal mol^{-1}), effectively ruling out this pathway (see supporting information). In order to gain further insight into role of the borane in the HDF of HFP, and the potential for alkene hydroboration in the mechanism, a series of stoichiometric experiments were conducted.

The 1:1 reaction of BH_3•L with HFP (L = NMe_3, THF, SMe_2) led to the clean formation of hydroborated intermediates **3•L** (Figure 4). For both L = THF and SMe_2 these reactions proceeded in high-yield allowing the *in-situ* generation of organoborane products as a single regioisomer. In contrast, for NMe_3 the reaction only proceeded in low conversion, consistent with the need for ligand dissociation prior to hydroboration. The intermediate **3•SMe$_2$** was characterised by the appearance of a diagnostic resonance in the ^{1}H NMR spectrum corresponding to the –CF_2H group at δ_H = 5.85 (ddd, $^2J_{HF}$ = 56.1, 54.0 Hz, $^3J_{HF}$ = 8.5 Hz) ppm. The data are consistent with formation of a single regioisomer and Markovnikov addition of the borane to HFP. While this intermediate could not be isolated due to its volatility, reaction of **3•SMe$_2$** with PPh_3 at 40 °C in toluene for 18 h cleanly generated the phosphine adduct, **3•PPh$_3$**, which can be isolated as a crystalline, colourless solid (Figure 4b). The crystal structure clearly shows the expected Markovnikov regioselectivity with no

evidence for the formation of the anti-Markovnikov isomer in this instance (Figure 4a). The P–B distance of 1.950(5) Å in **3•PPh$_3$** is unremarkable and slightly elongated over BH_3•PPh_3 (av. 1.917 Å). [18]

Reaction of BH_3•THF with a mixture of E-/Z-**2** (generated from the partial reduction of HFP by AlH_3•NMe_3 followed by vacuum transfer to remove the involatile inorganic side-products) also resulted in hydroboration generating **4•THF** which could be trapped as **4•PPh$_3$**. The major product is again that of Markovnikov addition. **4•PPh$_3$** is characterised by a distinct multiplet at δ_H ~ 4.50 ppm which could be modelled as the two diastereotopic ^{1}H environments of the –C(F)CF$\underline{H_2}$ group considered as an ABMX spin system insulated from the $–CF_3$ and B-containing moieties (Figure 4b). Equally diagnostic was the triplet resonance at δ_F = –220.55 (t, $^2J_{F\text{-}H}$ = 50.4 Hz) ppm in the ^{19}F NMR which collapsed to a singlet on proton decoupling. Despite **4•PPh$_3$** being the major product, it is not generated cleanly, in part this is due to the difficulty in the selective reduction of HFP to *E/Z*-**2**, which in our hands contains small amounts of HFP and HFO-1234yf. The analysis is further complicated by the realisation that *E*-**2** and *Z*-**2** would give rise to two possible diastereomers of the anti-Markovnikov isomer of **4•PPh$_3$**. Based on total integration of quantitative ^{19}F{^{1}H} NMR experiments it can be determined that Markovnikov **4•PPh$_3$** forms in at least 81 % yield giving a minimum selectivity of 4:1 for the major product. The true selectivity for the Markovnikov isomer is likely much higher.

Commercial samples of HFO-1234yf reaction with BH_3•THF to form an approximate 1:1 mixture of Markovinkov and anti-Markovinkov products **5•PPh$_3$,** following trapping with PPh_3. In this instance, the analysis is simplified due to the lower fluorine content of the substrate, along with its availability in high purity. Markovnikov **5•PPh$_3$** is characterised by a diagnostic doublet for the $–CH_3$ group δ_H = 1.58 (d, $^3J_{F–H}$ = 23.8 Hz) ppm, while the anti-Markovnikov isomer shows a distinct resonance at δ_H = 4.49 ppm which is assigned to the terminal proton of the $–CH_2C\underline{H}FCF_3$ moiety with appropriate coupling (Figure 4c). The assignments have been confirmed by ^{19}F, ^{19}F{^{1}H}, ^{1}H–^{1}H and ^{1}H–^{19}F NMR spectroscopy. In the case of the anti-Markovnikov product of **5•PPh$_3$** the data are further supported by a known germanium analogue $Et_3GeCH_2CHFCF_3$ formed from the hydrogermylation of HFO-1234yf under catalytic conditions.[19]

Figure 4. Reactions of BH_3•L with (a) HFP, (b) E/Z-**2** and (c) HFO-1234yf. Along with selected data that support the assignment of the products and regioselectivity of hydroboration. J values from simulated spectra. Peaks marked with an * are the impurity **4•PPh$_3$** in samples of **5•PPh$_3$**.

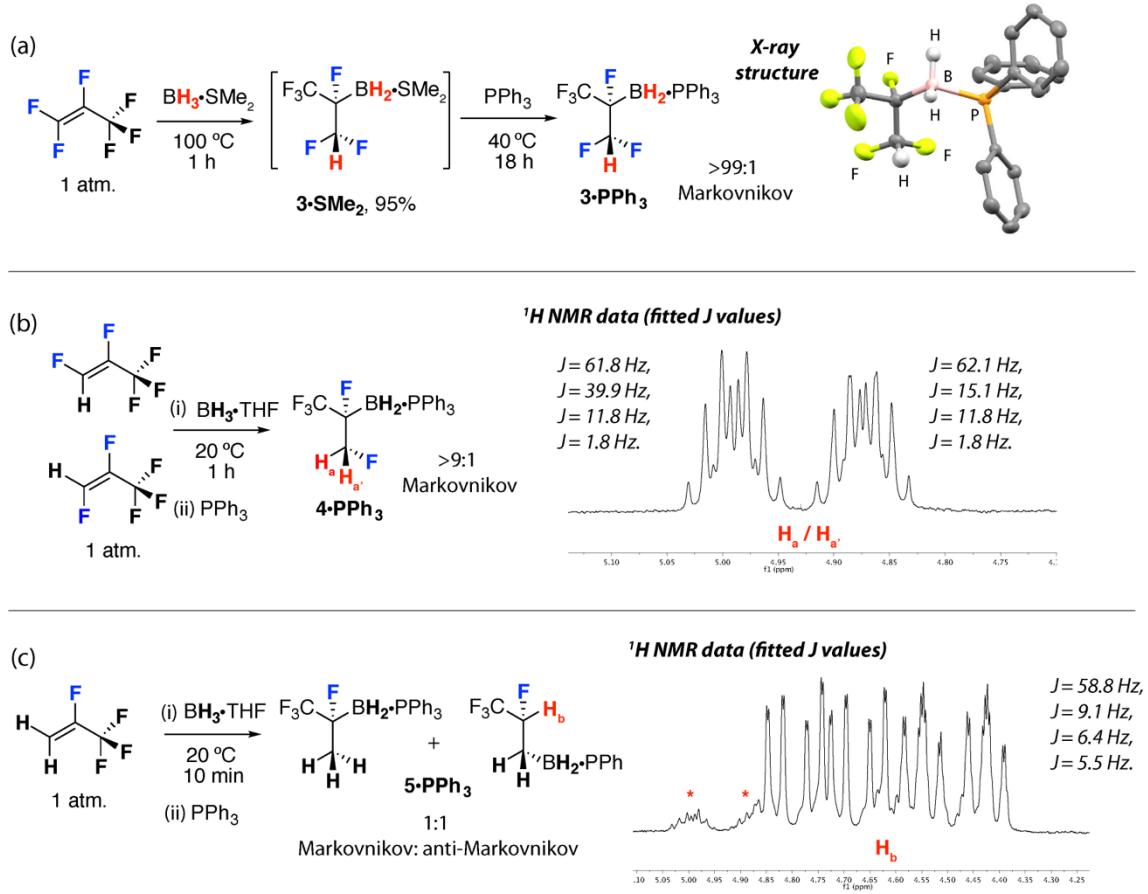

In combination, these reactions show that, while the hydroboration of HFP proceeds in high-selectivity, the regioselectivity is sensitive to the fluorine content of the olefin. Hence, although *E*-**2** and *Z*-**2** give predominantly Markovnikov products, HFO-1234yf reacts unselectively with both modes of addition of BH_3 to the olefin observed. Substituent effects on the regioselectivity of alkene hydroboration are well understood.[20-22] Expanding on the work of Stone,[13,23] Brown and co-workers have demonstrated previously that trifluoropropene reacts with HBX_2 (X = Cl, Br, H) to give primarily Markovnikov substitution products with the selectivity being sensitive to the number of halogen ligands on the borane and ranging from 7:1 to >9:1.[12] Similarly, vinyl chloride has been proposed to react with BH_3 by Markovnikov addition.[24] As with the cS_NV pathway, selectivity dictated by a combination of inductive (–F and $–CF_3$) and mesomeric effects (–F). The halogen containing groups primarily lead to stabilisation of the negative charge at the adjacent carbon centre in the transition state for hydroboration, and hence Markovnikov selectivity. For HFO-1234yf it would seem that the influence of the electron-withdrawing substituents is counter-balanced by the mesomeric effect of the sp^2 C–F moiety favouring the anti-Markovnikov addition and connection of the boron to a carbon atom that bears no fluorine atoms.

Accurate computation modelling of hydroboration pathways by DFT calculations is surprisingly complex. Due to the extremely low energy local barrier for the hydroboration step, Singleton and others have commented that the approximations of transition state theory may not hold.[25-27] Precise determination of the regioselectivity of the addition of boranes to even simple alkenes requires the consideration of reaction dynamics and modelling of reaction trajectories in place of more standard computational approaches.[28-30] As such, we are reluctant to use DFT calculations to model the complete reaction mechanism of the HDF of HFP with BH_3. The complexity described above is further confounded by the realisation that a mixture of reagents that may be involved in the HDF step, *viz* BH_3, BH_2F and BHF_2 which may perform the hydroboration step with different selectivities. [12] The concentrations of the latter boron fluorides are expected to increase at higher conversion.

What is clear from the experiments is that both Markovnikov and anti-Markovnikov products are accessible under the reaction conditions, with the selectivity for the major Markovnikov isomer decreasing with decreasing fluorine content of the olefin. Heating solutions of **3•SMe$_2$** in C_6D_6 led to slow HDF. Similarly, both **4•THF** and **5•THF** are competent reaction intermediates giving rise to HDF products. In the latter case it is notable that both Markovnikov and anti-Markovnikov isomers are consumed in the reaction to form predominantly 3,3,3-trifluoropropene.

Two potential mechanisms explain the observed intermediates and the selectivity for HFO-1234ze in the HDF of HFP. Both involve addition-elimination. A reaction sequence involving, Markovnikov addition / β-fluoride elimination followed by anti-Markovnikov addition / β-fluoride elimination would yield mixtures of *E/Z*-**2** and *E/Z*-HFO-1234ze with limited preference for the *E*- or *Z*-isomer as observed experimentally (Figure 5 – Pathway 1). Alternatively, Markovnikov hydroboration of HFP with BH_3 to generate **3** followed by intramolecular hydride / fluoride exchange and subsequent β-fluoride elimination would yield mixtures of *E/Z*-HFO-1234ze directly (Figure 5 – Pathway 2). While unusual, this type of intramolecular rearrangement has been proposed before.[24]

Figure 5. Plausible addition-elimination reaction mechanisms originating from hydroborated intermediate **3**.

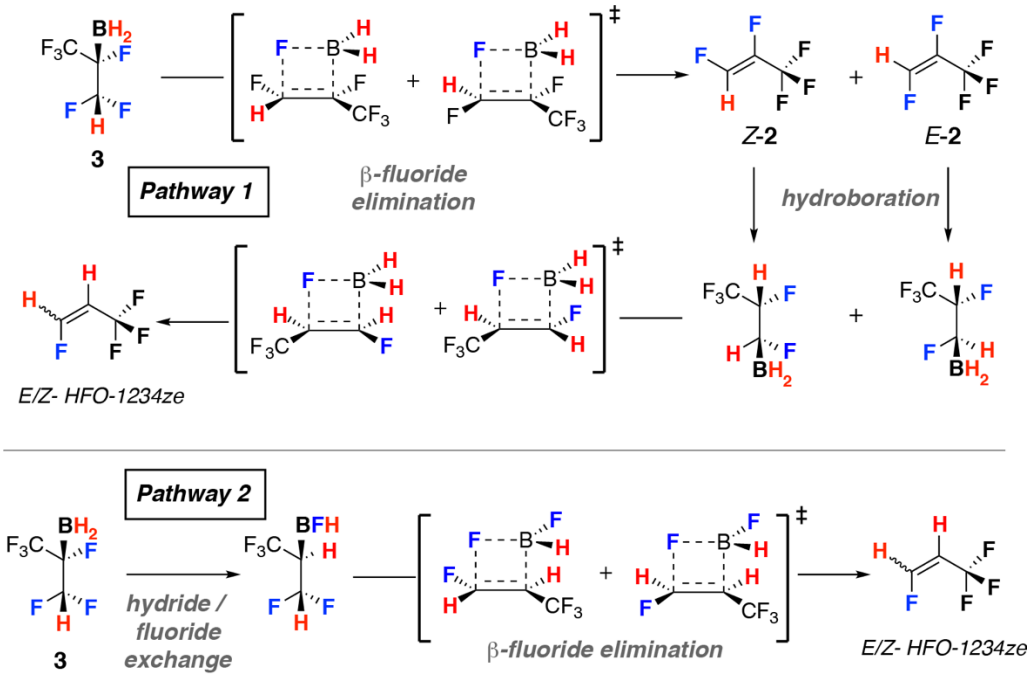

In order to probe the viability of these steps the local energy barriers for the β-fluoride elimination and hydride / fluoride exchange reactions were calculated by DFT (B3PW91 functional). Although the resulting data are of limited value in assessing the complete reaction sequence, they do provide some insight into whether these steps are accessible under the reaction conditions. β-Fluoride eliminations steps from either Markovnikov or anti-Markovnikov hydroborated intermediates **3** and **4** proceed with local Gibbs activation energies of $\Delta G^{\ddagger}_{298K}$ = 15 – 25 kcal mol^{-1}. The hydride / fluoride exchange mechanism originates from intermediate **2** which is formed exclusively as a single regioisomer based on the experimental data. The local Gibbs activation energy for the exchange transition state is $\Delta G^{\ddagger}_{298K}$ = 32.3 kcal mol^{-1}. This transition state involves a concerted migration of the hydride from boron-to-carbon and the fluoride from carbon-to-boron and develops cationic character on the carbon centre adjacent to boron.

Based on the calculations neither Pathway 1 nor Pathway 2 can be discounted at this stage. While it is possible that both may be operating under the reaction conditions (days at 100 °C) as Pathway 2 does not yield *E/Z*-**2** as intermediates it is unlikely to be the only mechanism in action. Experimentally *E/Z*-**2** mixtures were found to form Markovnikov hydroboration products with high selectivity, however the formation of a 1:1 mixture of regioisomers for HFO-1234yf shows that the selectively in these reactions is finely tuned. It is plausible that the substituted boranes BH_2F and

BHF_2 react with higher selectively for anti-Markovnikov addition favouring Pathway 1. Alternatively, the hydroboration step may be reversible and selectivity determined by the β-fluoride elimination step.

Conclusions

In summary, we report a new synthetic route to HFO-1234yf and HFO-1234ze that exploits the selective hydrodefluorination of hexafluoropropene. This method uses a bulk chemical commodity and does not rely on sequential chlorination and dichlorination sequences. Using main group hydrides of the form EH_3•L (E = B, L = SMe_2; E = Al, L = NMe_3) leads to complementary chemoselectivity in the hydrodefluorination sequence. With the borane reagent yielding a ~ 2:1 mixture of E- and Z-isomers of HFO-1234ze and the alane almost exclusively HFO-1234yf. The reaction by-products are boron and aluminium fluorides, compounds of commercial interest in their own right.

Exploration of the plausible reaction mechanisms by experiments and DFT calculations suggests that the complementary selectivities may have a mechanistic origin. For the alane, a concerted S_NV mechanism occurs with high substrate bias for H/F-exchange at the terminal position of HFP. For the borane, ligand dissociation followed by an addition elimination sequences proceeds with selectivity for H/F-exchange at the terminal and internal positions of HFP.

Our findings lay out an experimental and mechanistic template for the synthesis of modern refrigerants by a selective hydrodefluorination approach.

Conflicts of interest

Aspects of this work are the subject of UK patent application number 1810647.6 filed 28th June 2018 (one day before the 1st publication of ref. 14) in collaboration with Imperial Innovations.

Acknowledgements

We are grateful to the European Research Council (FluoroFix:677367) and the Royal Society (UF090149).

References

1 G. J. M. Velders, A. R. Ravishankara, M. K. Miller, M. J. Molina, J. Alcamo, J. S. Daniel, D. W. Fahey, S. A. Montzka and S. Reimann, *Science*, 2012, **335**, 922–923.

2 International Actions – The Montreal Protocol on Substances that Depelete the Ozone Layer, https://www.epa.govozone-layer-protectioninternational-actions-montreal-protocol-substances-deplete-ozone-layer. (accessed 5th Feb. 2019)

3 Eu legislation to control F-gases, https://www.ec.europa.eu/clima/policies/f-gas/legislation_en. (accessed 5th Feb. 2019)

4 Honeywell Blowing Agents, https://www.fluorineproducts-honeywell.com/blowingagents/regulation. (accessed 5th Feb. 2019)

5 H. K. Nair, R. R. Singh, A. J. Poss, D. Nalewajek, US Pat. 8889924B2, 2012; Honeywell International, Inc.

6 H. S. Tung, H. K. Nair, S. S. M. Mukhopadhyay, M. Van der Puy, WO Pat.2005108332A1, 2004, Honeywell International, Inc.

7 S. A. Cottrell, H. S. Tung, Y. C. Wang, G. Cerri, US Pat. 9255046B2, 2003, Honeywell International, Inc.

8 S. Lim, M. S. Kim, J.-W. Choi, H. Kim, B. S. Ahn, S. D. Lee, H. Lee, C. S. Kim, D. J. Suh, J.-M. Ha and K. H. Song, *Catalysis Today*, 2017, **293-294**, 42–48.

9 T. Braun, M. A. Salomon, K. Altenhöner, M. Teltewskoi and S. Hinze, 2009, **48**, 1818–1822.

10 T. Braun, F. Wehmeier and K. Altenhöner, 2007, **46**, 5321–5324.

11 P. V. Ramachandran, M. P. Jennings and H. C. Brown, *Org. Lett.*, 1999, **1**, 1399–1402.

12 H. C. Brown, G.-M. Chen, M. P. Jennings and P. V. Ramachandran, *Angew. Chem. Int. Ed.*, 1999, **38**, 2052–2054.

13 J. R. Phillips and F. G. A. Stone, *J. Chem. Soc.*, 1962, 94–97.

14 H. Schneider, A. Hock, A. D. Jaeger, D. Lentz and U. Radius, *Eur. J. Inorg. Chem.*, 2018, 4031–4043.

15 A. D. Jaeger, C. Ehm and D. Lentz, *Chem. Eur. J.*, 2018, **24**, 6769–6777.

16 H. C. Brown and J. Chandrasekharan, *J. Am. Chem. Soc.*, 1984, **106**, 1863–1865.

17 K. K. Wang and H. C. Brown, *J. Am. Chem. Soc.*, 1982, **104**, 7148–7155.

18 J. C. Huffman, W. A. Skupinski and K. G. Caulton, *Crystal Structure Communications*.

19 G. Meißner, K. Kretschmar, T. Braun and E. Kemnitz, *Angew. Chem. Int. Ed.*, 2017, **56**, 16338–16341.

20 H. C. Brown and G. Zweifel, *J. Am. Chem. Soc.*, 1960, **82**, 4708–4712.

21 G. D. Graham, S. C. Freilich and W. N. Lipscomb, *J. Am. Chem. Soc.*, 1981, **103**, 2546–2552.

22 H. C. Brown and A. W. Moerikofer, *J. Am. Chem. Soc.*, 1963, **85**, 2063–2065.

23 B. Bartocha, W. A. G. Graham and F. G. A. Stone, *J. Inorg. Nucl. Chem.*, 1958, **6**, 119–129.

24 D. J. Pasto and R. Snyder Sr., *J. Org. Chem.*, 1966, **31**, 2773–2777.

25 J. O. Bailey and D. A. Singleton, *J. Am. Chem. Soc.*, 2017, **139**, 15710–15723.

26 Y. Oyola and D. A. Singleton, *J. Am. Chem. Soc.*, 2009, **131**, 3130–3131.

27 D. R. Glowacki, C. H. Liang, S. P. Marsden, J. N. Harvey and M. J. Pilling, *J. Am. Chem. Soc.*, 2010, **132**, 13621–13623.

28 D. J. S. Sandbeck, C. M. Kuntz, C. Luu, R. A. Mondor, J. G. Ottaviano, A. V. Rayer, K. Z. Sumon and A. L. L. East, *J. Phys. Chem. A*, 2014, **118**, 11768–11779.

29 X. Wang, Y. Li, Y.-D. Wu, M. N. Paddon-Row, N. G. Rondan and K. N. Houk, *J. Org. Chem.*, 1990, **55**, 2601–2609.

30 M. J. S. Dewar and M. L. McKee, *Inorg. Chem.*, 2002, **17**, 1075–1082.